

PAPER

[View Article Online](#)
[View Journal](#) | [View Issue](#)

A green and facile approach for the synthesis of water soluble fluorescent carbon dots from banana juice

Cite this: *RSC Advances*, 2013, **3**, 8286

Bibekananda De and Niranjana Karak*

Green luminescent water soluble oxygenous carbon dots with an average size of 3 nm were synthesized by simply heating banana (*Musa acuminata*) juice at 150 °C for 4 h without using any surface passivating and oxidizing agent or inorganic salt. The literature was used to propose a possible mechanism for the formation of carbon dots by this approach. The resulting carbon dots exhibited concentration, excitation wavelength and pH dependent luminescent behavior in the visible range. The quantum yield was 8.95 on excitation at a wavelength of 360 nm, using quinine sulfate as the reference. The presence of large amounts of oxygenous functionality was confirmed by FTIR and EDX studies. XRD and TEM illustrated the poor crystalline nature and narrow distribution of these spherical carbon dots. Thus bio-based fluorescent carbon dots with a high yield were reported for the first time through a simple and effective route without using any special apparatus or reagents.

Received 8th January 2013,
Accepted 22nd March 2013

DOI: 10.1039/c3ra00088e

www.rsc.org/advances

Introduction

Fluorescent carbon dots, a young smart member of the carbon nanomaterial family, were first obtained during purification of single-walled carbon nanotubes in 2004.¹ They are generally oxygenous carbon nanoparticles with a size of less than 10 nm.² Carbon dots gradually became exciting nanomaterials because of their benign and inexpensive nature with ease of availability which resulted in their numerous possible applications in optoelectronic devices, biological labeling and biomedicines.^{2–5} Compared to traditional semiconductor quantum dots and organic dyes, photoluminescent carbon dots are superior in terms of aqueous solubility, functionalizability, resistance to photobleaching, toxicity and biocompatibility, though they exhibit broader photoluminescence profiles and a lower quantum yield (<3%).^{6–8} Thus several strategies have been demonstrated for the synthesis of carbon dots with desired properties. High energy ion beam radiation and laser ablation are two common approaches for the preparation of carbon dots from cement and graphite powders.^{7,9} However, to prevent the use of expensive precursors and energetic systems, different chemical methods are being adopted. Oxidation of gas soot, carbon soot or activated carbon using strong acids like nitric acid are also relatively inexpensive ways to prepare carbon dots,^{10,11} but the use of large amounts of such strong acids is undesirable and hazardous. Again, the carbonization of glucose, sucrose, glycol, glycerol, citric acid, ascorbic acid, *etc.* has achieved

significant attention for the production of fluorescent carbon dots. However most of these methods need multi-step operations and strong acids as well as post-treatment with surface passivating agents to improve the water solubility and luminescent properties of carbon dots.^{12–14} Recently, serious efforts are being made to obtain self-passivating carbon dots by one step hydrothermal carbonization with high temperature or microwave assisted hydrothermal carbonization of different carbon precursors.^{15–19} Again, all these methods also suffer from some drawbacks like the requirement of a complex and time consuming process, a high temperature and harsh synthetic conditions, hence these methods are highly expensive, which limits their wide applicability. Thus the production of carbon dots from renewable bio-precursors with inexpensive and greener methods is a challenging but worthy concept. Sahu *et al.* reported such an endeavor from a readily available natural bio-resource, orange peel.¹⁹ However, the yield of the carbon dots from this bio-resource was very low. Here, we report a facile and greener synthetic approach with a high yield of green fluorescent carbon dots by simply heating banana juice, a bio-resource, in a glass bottle. The formation of carbon dots and their luminescence behavior under various conditions were investigated. A detailed possible mechanism for the formation of the carbon dots from banana juice was also proposed by help of literature reports.

Experimental

Materials

Banana (*Musa acuminata*) was purchased from the local market of Assam, India. Ethanol (Merck, India) and quinine

Advanced Polymer and Nanomaterial Laboratory, Department of Chemical Sciences, Tezpur University, Napaam-784028, Tezpur, India.

E-mail: karakniranjan@yahoo.com; Fax: +91-3712-267006; Tel: +91-3712-267009

sulfate (Sigma-Aldrich, Germany) were used as received. All other chemicals used were of reagent grade.

Synthesis of carbon dots from banana juice

Carbon dots were synthesized by simply heating banana juice in a glass bottle. In a typical procedure, a banana (*ca.* 80 g) was cut into small pieces and turned into a paste with 100 mL of water. Then 20 mL of the juice (pulp-free, solid content 52 mg mL⁻¹) was taken with 20 mL of ethanol in a 60 mL glass bottle plugged with a cotton cork and heated at constant temperature of 150 °C in an oven for 4 h. A dark brown product was obtained after cooling at room temperature. This was dissolved in 20 mL of water and the residue was separated by filtration. 50 mL of ethanol was added into the aqueous filtrate and centrifuged at 960 × g (3000 rpm) for 15 min under ambient conditions to separate the large particles. The solvent was evaporated at room temperature under vacuum to obtain highly fluorescent carbon dots. The yield of the desired carbon dots was 600 mg (58% mass yield).

Characterization

The FTIR spectrum of the carbon dots was recorded on a Nicolet FTIR spectrophotometer (Impact-410, Madison, USA) using a KBr pellet. The elemental composition of the carbon dots was determined by electron dispersive X-ray study (EDX, JSM-6390LV). The amorphous nature and the interlayer spacing of the carbon dots were measured by an X-ray Diffractometer, Miniflex (Rigaku Corporation, Japan). The morphology and the microstructure of the carbon dots were analyzed by a high resolution transmission electron microscope, HRTEM (JEOL, JEMCXII, Transmission Electron Microscope operating voltage at 200 kV). A UV-visible absorption spectrum of the carbon dots in aqueous solution was recorded using a UV Spectrometer, Hitachi (U2001, Tokyo, Japan). The photoluminescent spectra were recorded using a photoluminescent setup (Perkinelmer Singapore PTE Ltd., Singapore, Model LS 55) in aqueous solution. The quantum yield of the carbon dots was determined at an excitation wavelength of 360 nm by the equation,

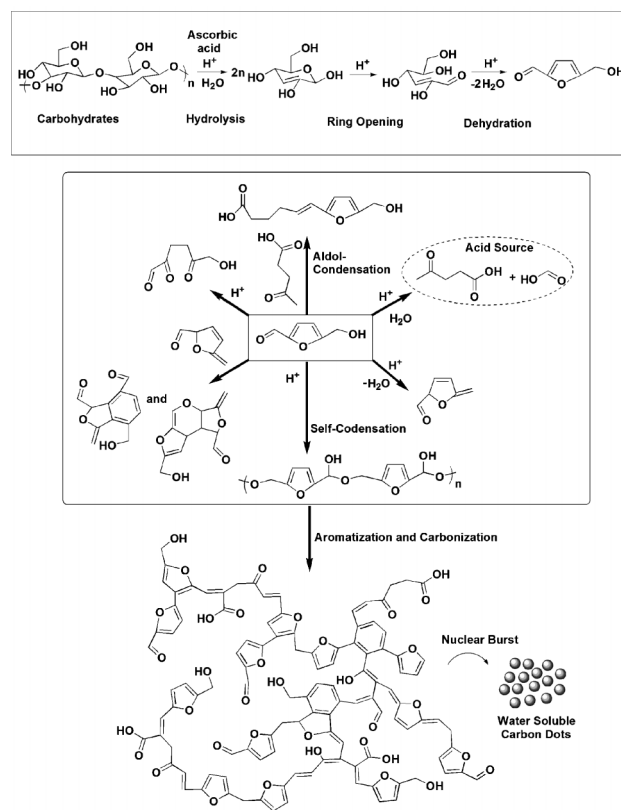
$$Q_{CD} = Q_R \cdot \frac{I_{CD}}{I_R} \cdot \frac{A_R}{A_{CD}} \cdot \frac{\eta_{CD}^2}{\eta_R^2} \quad (1)$$

where 'Q' is the quantum yield, 'I' is the intensity of luminescent spectra, 'A' is the absorbance at excited wavelength and 'η' is the refractive index of the solvent used; using quinine sulfate (quantum yield 54) in 0.1 M H₂SO₄ solution as the reference. The subscripts 'CD' for carbon dots and 'R' for reference are used in this equation.

Results and discussion

Synthesis and characterization of the carbon dots

Synthesis. Carbon dots were synthesized by carbonization of banana juice which contains carbohydrates like glucose, fructose, sucrose and ascorbic acid as the carbon precursors. Although the literature has reported the possible schematic route for the formation of carbon dots from carbon precursors,



Scheme 1 Possible mechanism for the formation of carbon dots.

obtained by the hydrothermal method,¹⁹ there is no clear and detailed mechanism for the same. Thus a detailed possible mechanism is proposed for the formation of carbon dots from banana juice as shown in Scheme 1 based on the literature reports of carbonization of carbohydrates.^{20–22} At first hydrolysis, dehydration and decomposition of different carbohydrates takes place in the presence of ascorbic acid and results in soluble compounds like furfural aldehydes, ketones and several organic acids like acetic, levulinic, formic acid, *etc.* which act as acid resources for different acid catalytic reactions (Scheme 1). Polymerization and condensation of these products transforms them into different soluble polymeric products. The aromatization and carbonization then take place *via* condensation and cycloaddition reactions (Scheme 1). Finally the carbon dots are obtained by a probable nuclear burst of these aromatic clusters at a critical concentration at the supersaturation point. Here, the presence of ascorbic acid in banana promotes the reaction at low temperature to occur within a short time. All the intermediates suggested by the mechanism are found in the literature. The final structure was also analyzed by FTIR, NMR and EDX studies.

Composition and structure. The formation of carbon dots with an average size of 3 nm was confirmed from TEM micrographs as shown in Fig. 1. The TEM images clearly reveal that the carbon dots are spherical in shape with a narrow size distribution ranging between 1.5 nm to 4.5 nm (Fig. 1b). These

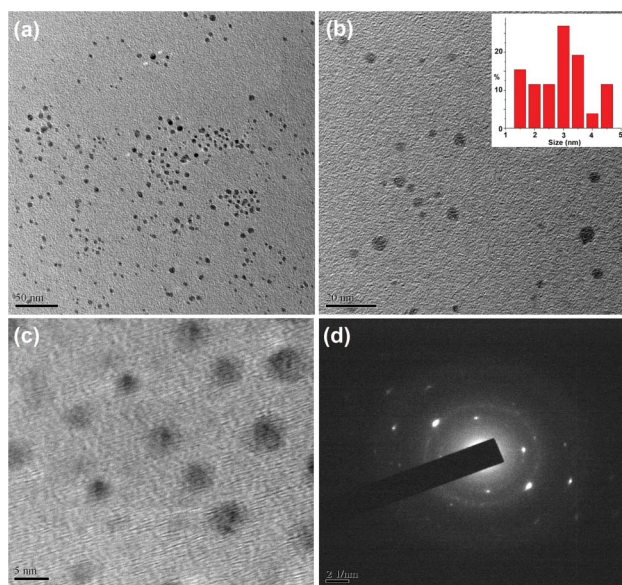


Fig. 1 TEM micrographs at different magnifications (a) 50 nm (b) 20 nm (with size distribution, inset) and (c) 5 nm, and (d) SAED pattern of the carbon dots.

finer particles with a narrow size distribution are plausible due to the use of milder conditions compared to literature reports. In order to determine the elemental composition, the weight and atomic ratios of C and O of the carbon dots were estimated from EDX data (Fig. 2a) and were found to be 63.39 : 35.69 and 70.07 : 29.61 respectively. A minor amount (0.92% in weight or 0.31% in atomic ratio) of potassium was also found due to the use of bananas, which contain this element. The different oxygenous functional groups and

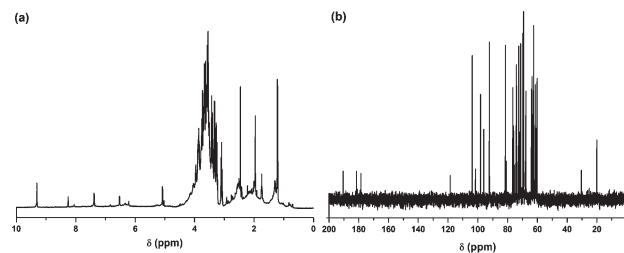


Fig. 3 (a) ^1H -NMR and (b) ^{13}C -NMR spectra of the carbon dots.

linkages in the carbon dots were evident by FTIR data (Fig. 2c). In this spectrum stretching frequencies at 3492, 2935, 1730, 1625, 1422, 1264 and 918 cm^{-1} indicated the presence of $-\text{OH}$, $-\text{C}-\text{H}$, $\text{C}=\text{O}$, $\text{C}=\text{C}$, $\text{C}-\text{O}-\text{C}$, $\text{C}-\text{O}$ and an epoxy ring respectively. The presence of these functional groups suggests that the synthesized carbon dots have excellent water solubility. The NMR spectra (Fig. 3) reveal the presence of four different kinds of chemical environments in the four different regions as discussed below.² In the ^1H NMR spectrum (Fig. 3a) the regions found are: 1–3 ppm (for sp^3 $\text{C}-\text{H}$ protons), 3–6 ppm (for the protons attached with hydroxyl, ether and carbonyl groups), 6–8 ppm (for the aromatic or sp^2 protons) and 8–10 ppm (for the aldehydic protons). Also in the ^{13}C NMR spectrum (Fig. 3b), four similar regions *viz.* 20–80 ppm (for sp^3 carbons and carbons attached with hydroxyl groups), 80–100 ppm (for carbons attached with ether linkages), 100–120 ppm (for $\text{C}=\text{C}$ aromatic or sp^2 carbons) and 175–190 ppm (for $\text{C}=\text{O}$ carbons) are found. The XRD pattern (Fig. 2b) of the carbon dots shows a broad peak at 21.1° corresponding to the (002) peak. This indicates the interlayer spacing (d) of the carbon dots (0.42 nm) is higher than that of the graphitic interlayer spacing (0.33 nm) along with the broadness character. This confirms the poor crystalline nature of carbon dots, which is attributed to the generation of more oxygen containing groups. This is further confirmed by the selected-area electron diffraction (SAED) pattern of the carbon dots as shown in Fig. 1d.

Absorbance and luminescence properties

The optical absorption peak of the carbon dots was observed in the UV region with a maximum absorption at 283 nm and a tail extending into the visible range (Fig. 4a). This is attributed to the $n-\pi^*$ transition of the $\text{C}=\text{O}$ band and $\pi-\pi^*$ transition of the conjugated $\text{C}=\text{C}$ band.

The classic signature of carbon dots is emission wavelength and size dependent photoluminescent behavior. From the fundamental as well as application viewpoint, PL is one of the most fascinating behaviors of carbon dots. The synthesized carbon dots in aqueous solution show green luminescence on exposure of UV light as shown in the inset of Fig. 4a. From the photoluminescent spectra of the carbon dots (Fig. 4b) it was clear that the PL intensity is dependent on the concentration of the carbon dots. The intensity of the PL spectra sharply increases with decreasing concentration of carbon dots. This may be due to decreasing interactions among the different polar groups at low concentrations. The presence of a high

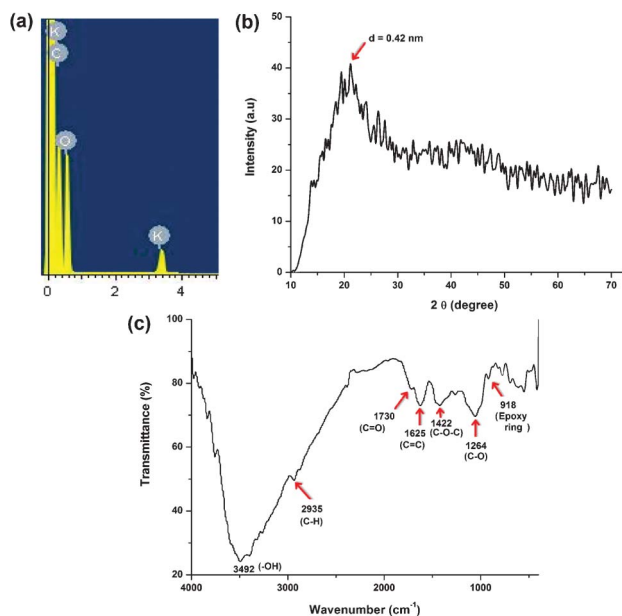


Fig. 2 (a) EDX spectrum, (b) XRD pattern and (c) FTIR spectrum of the carbon dots.

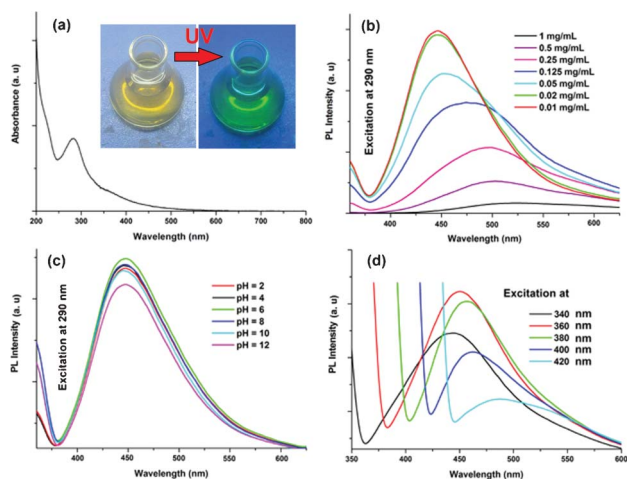


Fig. 4 Spectra of the carbon dots: (a) UV absorption, and PL with variation of (b) concentration, (c) pH and (d) excitation wavelength (340–420 nm).

amount of polar functionality helps to form agglomeration at high concentrations. The PL intensity is also dependent on the excitation wavelength. The PL spectra of carbon dots with variation of excitation wavelength (340–420 nm) are shown in Fig. 4d. A strong PL emission peak located at 460 nm was observed with an excitation wavelength of 360 nm. The emission peak was also shifted to a higher wavelength with the increase of the excitation wavelength, which is shown clearly in Fig. 5. The mechanism of the PL behavior of carbon dots is very complicated and has not yet been clearly reported. The plausible reasons for the PL behavior are the presence of different particle sizes and the distribution of the different surface energy traps of the carbon dots.¹⁹ The difference in the position of emission peak is due to the variation in size of the carbon dots. The energy gap increases with the decrease in size of the carbon dots and *vice versa* due to the quantum confinement effect like semiconductor quantum dots. Thus

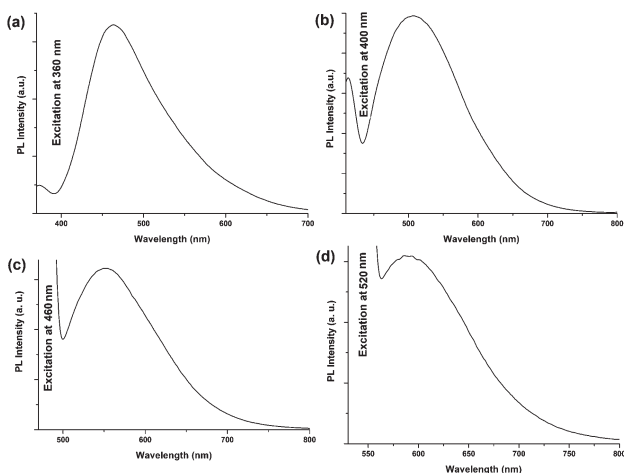


Fig. 5 PL emission spectra of carbon dots at (a) 360 nm, (b) 400 nm, (c) 460 nm and (d) 520 nm excitation wavelengths.

the particles with a smaller size get excited at a lower wavelength, whereas those with a larger size get excited at higher wavelengths. The intensity of the PL depends on the number of particles excited at a particular wavelength. The highest PL intensity of carbon dots was observed at an excitation wavelength of 360 nm, due to the largest number of particles being excited at that wavelength. Another reason for the excitation dependent PL behavior of carbon dots is the nature of their surface. The presence of various functional groups on the surface of the carbon dots may result in a series of emissive traps between π and π^* of C–C. On illuminating the carbon dots at a certain excitation wavelength a surface energy trap dominates the emission. As the excitation wavelength changes, other corresponding surface state emissive traps become dominant. Hence the PL mechanism is controlled by both the size effects and surface defects. In Fig. 4c the variation of PL intensity with pH (2–12) is shown. A strong PL intensity was observed in the physiological pH range (4–8). This is due to the electronic transitions of π – π^* and n – π^* that are changed by refilling or depleting their valance bands with the variation in pH.² Using quinine sulfate as a reference quantum yield of carbon dots in aqueous solution as measured at an excitation wavelength of 360 nm and was found to be 8.95. This value is higher than the literature reported values for non-passivating carbon dots. Thus the PL characteristic of the prepared carbon dots is promising for their different possible applications. In biological detection, carbon dots can be applied at low concentrations as the PL intensity is sensitive to the concentration of carbon dots whereas at low concentration the variation of PL intensity is negligible. In addition, the PL is also sensitive to the excitation wavelength, which may also pose a problem in biological detection. This is due to the wide size distribution of the

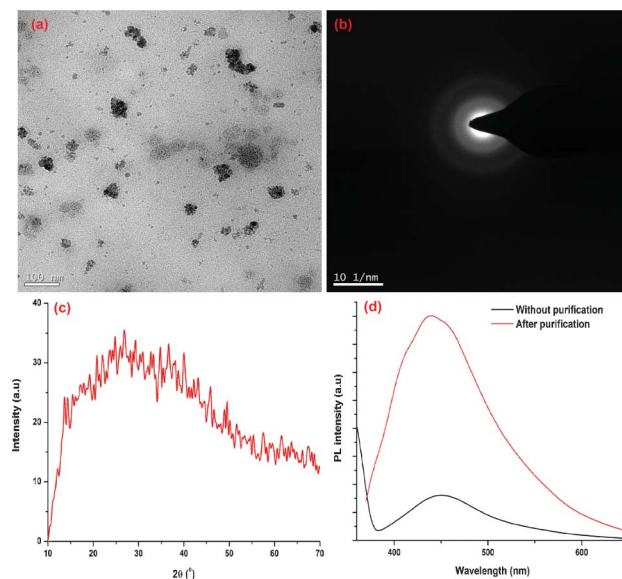


Fig. 6 (a) TEM image, (b) SAED and (c) XRD patterns of the carbon dots with coarse carbon nanoparticles; (d) PL spectrum of carbon dots in the presence/absence of coarse carbon particles.

carbon dots which can be solved by preparing monodispersed carbon dots using a properly designed protocol.

The variation of crystallinity and PL behavior of the carbon dots in the presence of coarse carbon particles is shown in the Fig. 6. Both PL and crystallinity are sharply decreased for the un-purified carbon dots compared to the purified carbon dots. This is comparable with the literature value.¹⁹ The TEM image of the un-purified carbon dots shows the presence of coarse carbon nanoparticles (Fig. 6a).

Conclusions

So, in this study, we have demonstrated a facile, simple and large scale synthesis of water soluble green fluorescent carbon dots from a cheap and readily available natural precursor. They exhibited interesting concentration, pH and excitation wavelength dependent photoluminescent behavior in the visible range with a high quantum yield. So these bio-based and water soluble highly luminescent carbon dots can potentially be applied in solution state optoelectronics.

Acknowledgements

The authors express their gratitude to the NRB for financial assistance through grant no. DNRD/05/4003/NRB/251 dated 29.02.12, SAP (UGC), India through grant no. F.3-30/2009(SAPII) and the FIST program-2009 (DST), India through grant no. SR/FST/CSI-203/209/1 dated 06.05.2010. SAIF, NEHU, Shillong is gratefully acknowledged for the TEM imaging.

References

- 1 X. Xu, R. Ray, Y. Gu, H. J. Ploehn, L. Gearheart, K. Raker and W. A. Scrivens, *J. Am. Chem. Soc.*, 2004, **126**, 12736–12737.
- 2 X. Jia, J. Li and E. Wang, *Nanoscale*, 2012, **4**, 5572–5575.
- 3 Q. Li, T. Y. Ohulchanskyy, R. Liu, K. Koyanov, D. Wu, A. Best, R. Kumar, A. Bonoiu and P. N. Prasad, *J. Phys. Chem. C*, 2010, **114**, 12062–12068.
- 4 E. J. Goh, K. S. Kim, Y. R. Kim, H. S. Jung, S. Beack, W. H. Kong, G. Scarcelli, S. H. Yun and S. K. Hahn, *Biomacromolecules*, 2012, **13**, 2554–2561.
- 5 S. T. Yang, L. Cao, P. G. Luo, F. Lu, X. Wang, H. Wang, M. J. Mezziani, Y. Liu, G. Qi and Y. P. Sun, *J. Am. Chem. Soc.*, 2009, **131**, 11308–11309.
- 6 P. C. Hsu, Z. Y. Shih, C. H. Lee and H. T. Chang, *Green Chem.*, 2012, **14**, 917–920.
- 7 H. Li, Z. Kang, Y. Liu and S. T. Lee, *J. Mater. Chem.*, 2012, **22**, 24230.
- 8 X. Wang, K. Qu, B. Xu, J. Rena and X. Qu, *J. Mater. Chem.*, 2011, **21**, 2445–2450.
- 9 Y. P. Sun, B. Zhou, Y. Lin, W. Wang, K. A. S. Fernando, P. Pathak, M. J. Mezziani, B. A. Harruff, X. Wang, H. Wang, P. G. Luo, H. Yang, M. E. Kose, B. Chen, L. M. Veca and S. Y. Xie, *J. Am. Chem. Soc.*, 2006, **128**, 7756–7757.
- 10 H. Liu, T. Ye and C. Mao, *Angew. Chem., Int. Ed.*, 2007, **46**, 6473–6475.
- 11 Z. A. Qiao, Y. Wang, Y. Gao, H. Li, T. Dai, Y. Liua and Q. Huo, *Chem. Commun.*, 2010, **46**, 8812–8814.
- 12 J. Zhang, W. Shen, D. Pan, Z. Zhang, Y. Fang and M. Wu, *New J. Chem.*, 2010, **34**, 591–593.
- 13 N. Puvvada, B. N. P. Kumar, S. Konar, H. Kalita, M. Mandal and A. Pathak, *Sci. Technol. Adv. Mater.*, 2012, **13**, 045008.
- 14 X. Zhai, P. Zhang, C. Liu, T. Bai, W. Li, L. Dai and W. Liu, *Chem. Commun.*, 2012, **48**, 7955–7957.
- 15 Z. C. Yang, M. Wang, A. M. Yong, S. Y. Wong, X. H. Zhang, H. Tan, A. Y. Chang, X. Li and J. Wang, *Chem. Commun.*, 2011, **47**, 11615–11617.
- 16 P. C. Hsu and H. T. Chang, *Chem. Commun.*, 2012, **48**, 3984–3986.
- 17 Y. Yang, J. Cui, M. Zheng, C. Hu, S. Tan, Y. Xiao, Q. Yanga and Y. Liu, *Chem. Commun.*, 2012, **48**, 380–382.
- 18 Z. Zhang, J. Hao, J. Zhang, B. Zhang and J. Tang, *RSC Adv.*, 2012, **2**, 8599–8601.
- 19 S. Sahu, B. Behera, T. K. Maiti and S. Mohapatra, *Chem. Commun.*, 2012, **48**, 8835–8837.
- 20 M. M. Titirici, M. Antonietti and N. Baccile, *Green Chem.*, 2008, **10**, 1204–1212.
- 21 C. Falco, N. Baccile and M. M. Titirici, *Green Chem.*, 2011, **13**, 3273–3281.
- 22 J. Ryu, Y. W. Suh, D. J. Suh and D. J. Ahn, *Carbon*, 2010, **48**, 1990–1998.